Journal Pre-proof

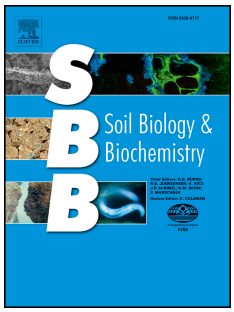

Microbial potential for denitrification in the hyperarid Atacama Desert soils

Di Wu, Mehmet Senbayram, Ghazal Moradi, Ramona Mörchen, Claudia Knief, Erwin Klumpp, Davey L. Jones, Reinhard Well, Ruirui Chen, Roland Bol

PII: S0038-0717(21)00121-8

DOI: https://doi.org/10.1016/j.soilbio.2021.108248

Reference: SBB 108248

To appear in: *Soil Biology and Biochemistry*

Received Date: 3 November 2020

Revised Date: 3 March 2021

Accepted Date: 3 April 2021

Please cite this article as: Wu, D., Senbayram, M., Moradi, G., Mörchen, R., Knief, C., Klumpp, E., Jones, D.L., Well, R., Chen, R., Bol, R., Microbial potential for denitrification in the hyperarid Atacama Desert soils, *Soil Biology and Biochemistry*, https://doi.org/10.1016/j.soilbio.2021.108248.

Microbial potential for denitrification in the hyperarid Atacama Desert soils

Di Wu[a], Mehmet Senbayram[b,c], Ghazal Moradi[d], Ramona Mörchen[e], Claudia Knief[f], Erwin Klumpp[d], Davey L. Jones[f,g], Reinhard Well[b], Ruirui Chen[h,*], Roland Bol[d]

[a]*Beijing Key Laboratory of Biodiversity and Organic Farming, College of Resources and Environmental Sciences, China Agricultural University, Beijing 100083, China*

[b]*Thünen Institute of Climate-Smart Agriculture, Bundesallee 65, Braunschweig 38116, Germany*

[c]*Institute of Plant Nutrition and Soil Science, University of Harran, Osmanbey, San-liurfa 63000, Turkey*

[d]*Institute of Bio- and Geosciences, Agrosphere (IBG-3), Forschungszentrum Jülich GmbH, Jülich 52425, Germany*

[e]*Soil Science & Soil Ecology, Institute of Crop Science and Resource Conservation (INRES), University of Bonn, Bonn 53115, Germany*

[f]*Institute of Crop Science and Resource Conservation, Molecular Biology of the Rhizosphere, University of Bonn, Bonn 53115, Germany*

[f]*Environment Centre Wales, Bangor University, Gwynedd, LL57 2UW, UK*

[g]*UWA School of Agriculture and Environment, University of Western Australia, Perth, WA 6009, Australia*

[h]*State Key Laboratory of Soil and Sustainable Agriculture, Institute of Soil Science, Chinese Academy of Sciences, Nanjing 210008, China*

[*]**Corresponding author:** Ruirui Chen

Tel.: +0086-25-86881345

E-mail: rrchen@issas.ac.cn

25

Abstract

The hyperarid soils of the Atacama Desert, Chile, contain the largest known nitrate deposits in the world. They also represent one of the most hostile environments for microbial life anywhere in the terrestrial biosphere. Despite known for its extreme dryness, several heavy rainfall events causing localised flash flooding have struck Atacama Desert core regions during the last five years. It remains unclear, however, whether these soils can support microbial denitrification. To answer this, we sampled soils along a hyperaridity gradient in the Atacama Desert and conducted incubation experiments using a robotized continuous flow system under a He/O_2 atmosphere. The impacts of four successive extreme weather events on soil-borne N_2O and N_2 emissions were investigated, i) water addition, ii) NO_3^- addition, iii) labile carbon (C) addition, and iv) oxygen depletion. The ^{15}N-N_2O site-preference (SP) approach was further used to examine the source of N_2O produced. Extremely low N_2O fluxes were detected shortly after water and NO_3^- addition, whereas pronounced N_2O and N_2 emissions were recorded after labile-C (glucose) amendment in all soils. Under anoxia, N_2 emissions increased drastically while N_2O emissions decreased concomitantly, indicating the potential for complete denitrification at all sites. Although increasing aridity significantly reduced soil bacterial richness, microbial potential for denitrification and associated gene abundance (i.e., *napA*, *narG*, *nirS*, *nirK*, *cnorB*, *qnorB* and *nosZ*) was not affected. The N_2O ^{15}N site preference values based on two end-member model suggested that fungal and bacterial denitrification co-contributed to N_2O production in less arid sites, whereas bacterial denitrification dominated with increasing aridity. We conclude that soil denitrification functionality is preserved even with lowered microbial richness in the extreme hyperarid Atacama Desert. Future changes in land-use or extreme climate events therefore have a potential to

destabilize the immense reserves of nitrate and induce significant N_2O losses in the region.

Keywords: Denitification; Greenhouse gases; Nitrogen cycling; Moisture status; Xerophile

1. Introduction

The Atacama Desert represents one of the most hostile environments for microbial life on Earth due to its hyperarid moisture regime, thermal extremes, high concentrations of salt in the soil, and intense UV radiation at the soil surface (Armando Azua-Bustos et al., 2012; Calderón et al., 2014). This makes the Atacama Desert an ideal location to study the potential for life to exist on other planets, e.g. Mars, which are thought to possess similar soil properties (McKay et al., 2003; Valdivia-Silva et al., 2012). Nevertheless, the Atacama Desert is not totally devoid of life. Short term water inputs caused by fog or rare rainfall events may provide temporary favourable conditions for microorganisms and plants (i.e. “desert blooms”; Orlando et al., 2010). Recent studies have shown that microbial communities in these soils respond rapidly to the addition of available carbon (C) when moisture limitation is removed (Jones et al., 2018). Conversely, the addition of water has also been shown to compromise organisms adapted to a xerophilic lifestyle (Azua-Bustos et al., 2018).

Biological denitrification, which is the major nitrogen (N) loss mechanism in terrestrial ecosystems, occurs via the sequential reduction of NO_3^- to NO_2^-, NO, N_2O and N_2 (Firestone, 1982). Denitrification was generally considered to be a prokaryotic process for a century, while it becomes clear nowadays that both bacteria and fungi possess the ability to produce N_2O during denitrification (Philippot et al., 2007; Laughlin and Stevens, 2002). Nevertheless, the relative contribution of fungi to soil

N_2O production remains poorly understood, especially in natural ecosystems (Senbayram et al., 2018; Xu et al., 2019). Although the occurrence of denitrification is widespread in moist soils, its functional significance in hyperarid ecosystem remains unknown. In the last five years, several extreme rainfall events occurred in the Atacama Desert, causing localised flash flooding (Wilcox et al., 2016; Azua-Bustos et al., 2018; Schulze-Makuch et al., 2018). Since the Atacama Desert contains the largest known nitrate deposits in the world, the susceptibility of these reserves to denitrification after land-use change or extreme climate events remains unclear (Michalski et al., 2004; Walvoord et al., 2003). Despite the fact that microbial communities in the Atacama Desert are of low abundance and low diversity, recently denitrification–related genes were detected (Knief et al., 2020; Orlando et al., 2012). Nevertheless, it is still not clear whether the environmental conditions in the Atacama Desert can support denitrifier activity, or whether those denitrification–related genes were introduced by atmospheric long-distance transport and deposition of bacterial cells (Mayol et al., 2017). In this study, we hypothesized that i) soils along a hyperarid gradient in the Atacama region will differ in microbial community composition, driven by differences in moisture availability; (ii) the capacity for complete denitrification will be preserved in the Atacama Desert soils but will decline with increasing aridity; ii) the response of denitrification-derived N_2O and N_2 emissions to highly ephemeral weather events (i.e. rainfall) will be slow and that this response will be bacterially driven.

The combination of a $\delta^{18}O$ and site preference ($\delta^{15}N^{sp}$) approach has been widely used during the last decade to distinguish the different sources of N_2O production pathways [+34‰ to +40‰ for nitrification (Ni) and fungal denitrification (fD), -9‰ to +9‰ for bacterial denitrification (bD)] (Decock and Six, 2013; Toyoda et al.,

2017). In this study we combined this isotopic mapping approach with qPCR and high-throughput 16S rRNA gene sequencing to (i) quantify rates of denitrification in a contrasting range of hyperarid soils, (ii) measure the abundance of functional genes involved in denitrification, (iii) determine whether denitrification could be attributed to fungi or bacteria, (iv) identify key abiotic factors that may limit denitrification, and (v) evaluate the theoretical potential for microbial-mediated loss of nitrate reserves in the Atacama region.

2. Materials and methods

2.1. Soil

Field sampling was undertaken in the Paposo transect of the Atacama Desert, Chile, in October, 2016 (Jones et al., 2018). The transect crosses a fog-nourished zone (Loma) at the coast before expanding into the hyperarid core of the desert at higher altitudes. Soil samples (0-10 cm) were collected from five sites under different levels of hyperaridity along an altitudinal transect near Paposo, Chile (Table 1). Mean annual temperature (MAT) ranges from 16.7 to 18.1 °C and mean annual precipitation (MAP) from 0 to 6.7 mm (Quade et al., 2007). The samples from all sites had a low intrinsic moisture content at the time of collection (20.4 ± 4.1 mg g^{-1}). Considering the spatial heterogeneity of the individual sites, soils were sampled from three independent spots located at least 20 m apart. All samples were homogenised by sieving (<2 mm) and stored in sealed sterile tubes to avoid contamination prior to use. Based on their moisture regime, the sites were divided into three levels of aridity, namely, semi-arid/arid (A1042), arid (A1243 and A1700) and hyperarid (A2029 and A2116).

126 *2.2. Automated soil incubation experiment and trace gas measurements*

127 The incubation experiment was carried out at Thünen Institute Braunschweig,
128 Germany, in a ROFLOW system using a He/O_2 atmosphere. The system and setup
129 have been described previously (Senbayram et al., 2018) and thus only a brief
130 overview will be given here. For each sample, 460 g of dry soil was packed into an
131 acrylic glass vessel (140 mm diameter and 150 mm height). All the vessels and
132 operational tools were ethanol-sterilized. Four successive events were simulated: i)
133 water addition, which can be induced by occasional fog and/or rare rainfall events
134 (Uritskiy et al., 2019); ii) NO_3^- addition, which can be induced by atmospheric
135 deposition (Reich and Bao, 2018); iii) available carbon (C) addition, which can be
136 induced by the wind-blown deposition of plant residues and the *in-situ* death of
137 microbial cells (Jones et al., 2018); iv) oxygen depletion, which may occur shortly
138 after extreme rainfall events.

139 The repacked soil core was submerged from the bottom of the vessel with sterile
140 water and drained to *ca* 23.0% gravimetric water content by applying a vacuum to the
141 ceramic plate (pore size 0.16 µm) at the base of the core. The incubation vessels were
142 then sealed and the atmospheric air in the vessels was replaced by pure He (≥99.999%
143 He) via applying vacuum from the top and filling with He in three cycles.
144 Subsequently, the vessel headspace was continuously flushed with a He and O_2 (80:20
145 v/v) mixture at a flow rate of ca. 25 mL min^{-1}. At day 34 and day 37, 20 mL of KNO_3
146 solution (equivalent to 6 mg N kg^{-1} dry soil) and 5 mL of glucose solution (equivalent
147 to 500 mg C kg^{-1} dry soil) was added, respectively, from the bottom of the vessel to
148 simulate N and C addition scenarios. At day 54, the atmospheric O_2 concentration was
149 adjusted to zero to create anoxic incubation conditions. The temperature of the
150 incubation room was set at 20 °C. The gas concentrations (N_2O, N_2, CO_2 and O_2) in

each vessel were analysed online via directing the outlet of each vessel sequentially to a gas chromatograph by two multi-positional valves (VICI, Houston, USA).

2.3. Soil sample collection and mineral N analyses

Soil samples of about 15 g were collected from each vessel at the beginning and the end of the incubation period. The soil samples were immediately frozen in liquid nitrogen and stored at -80°C. For mineral N analyses, the soil samples were extracted with 2 M KCl (1:5 w/v) by shaking for 1 h. The extracts were then filtered through Whatman 602 filter papers and stored at -20°C until analysis. The concentrations of NH_4^+ and NO_3^- in the soil extracts were measured using a continuous flow analyser (Smartchem 200S/N1104238, Westco, France).

2.4. Isotope analysis and N_2O source partitioning

Additional gas samples for isotopic analyses were taken from each incubation vessel by attaching 120-mL serum bottles to the outlet's inflow-through mode for around 2 h (Wu et al., 2017). The N_2O $\delta^{15}N^{bulk}$, $\delta^{15}N^{\alpha}$, and $\delta^{18}O$ isotope signatures were then determined by analysing *m/z* 44, 45, and 46 of intact N_2O^+ molecular ions, and *m/z* 30 and 31 of NO^+ fragment ions (Toyoda and Yoshida, 1999) on an isotope ratio mass spectrometer (Thermo Fisher Scientific, Bremen, Germany) at Thünen Institute Braunschweig, Germany (Köster et al., 2015). The initial substrate (SP_0) was calculated using a Rayleigh-type mode for samples in which both N_2O and N_2 concentrations were determined, assuming that isotope dynamics followed closed-system behaviour (Lewicka-Szczebak et al., 2014). For samples where the $N_2O/(N_2O+N_2)$ product ratio could not be determined (when N_2 concentrations were lower than detection limit (ca. 5 ppm)), a $\delta^{15}N^{sp}/\delta^{18}O$ mapping model was used to calculate the SP_0 (Wu et al., 2019). Distinguishing the N_2O produced by nitrification

and fungal denitrification based on SP values is impossible because of the overlapping SP signature from those pathways (Frame and Casciotti, 2010; Toyoda et al., 2017). Therefore, for source partitioning the endmember model was defined as 37‰ for nitrification/fungal denitrification, and –5‰ for bacterial denitrification (Toyoda et al., 2017) (see Supplementary material for further details of the calculation).

2.5. High-throughput sequencing of 16S rRNA gene amplicons

Genomic DNA was extracted from 0.5 g of soil using a FastDNA SPIN Kit for soil (MP Biomedicals, Santa Ana, CA). Negative controls were conducted by replacing soil samples with 0.5 g of water. The extracted DNA was dissolved in 50 µL TE buffer, evaluated using a NanoDrop 2000 (ThermoFisher, USA) and stored at -20°C until further use.

High-throughput sequencing of 16S rRNA genes was performed to analyse the bacterial community composition. PCR amplification was conducted for bacteria with primer set 519F/907R. The 5-bp barcoded oligonucleotides were fused to the forward primer. PCR was carried out in a 50-µL reaction mixture, containing deoxynucleoside triphosphates at a concentration of 1.25 µM, 2 µL (15 µM) forward and reverse primers, 2 U of Taq DNA polymerase (TaKaRa, Japan), and each reaction mixture received 2 µL of genomic DNA as a template. PCR reactions were performed according to the following program: 94 °C for 5 min, 30 cycles (94 °C for 30 s, 55 °C for 30 s, 72 °C for 45 s), and a final extension at 72 °C for 10 min. Reaction products for each soil sample were purified using the QIAquick PCR Purification kit (Qiagen, Hilden, Germany), and quantified using a NanoDrop ND-2000. The bar-coded PCR products from all samples were pooled at equimolar concentrations before sequencing.

High-throughput sequencing was performed using the Illumina Miseq sequencing platform (Illumina Inc., San Diego, CA) (Feng et al., 2018). After sequencing, 16S rRNA gene sequence data were processed using the Quantitative Insights Into Microbial Ecology (QIIME) data pipeline (Caporaso et al., 2010). Sequences with a quality score below 25 and the length fewer than 200 bp were trimmed and then assigned to soil samples based on the unique barcodes. Sequences were binned into OTUs using a 97% identity threshold, and the most abundant sequence from each OTU was selected as a representative sequence. Taxonomy was then assigned to OTUs with reference to a subset of the SILVA 119 database (http://www.arb-silva.de/download/archive/qiime/). All samples were then rarefied to 150,000 sequences per sample to evaluate bacterial diversity, which allowed us to compare general diversity patterns among treatments.

2.6. High-throughput quantitative PCR

The abundance of functional genes involved in the N cycle were estimated by high-throughput quantitative PCR (HT-qPCR, SmartChip Real-time PCR system, WaferGen Biosystems Inc., Fremont, USA), adapted from Zhu et al. (2017) and Zheng et al. (2018). A total of 36 primer sets were used including the 16S rRNA gene (F519/R907) as a reference gene. According to the manufacturer's instructions (SmartChip^{TM} MyDesign Kit User Manual; Takara Bio USA Inc., Mountain View, CA), PCR primers and DNA samples were loaded into two subarrays with corresponding reagents, respectively. The thermal program consisted of an initial denaturation at 95 °C for 10 min, followed by 42 cycles of denaturation at 95 °C for 34 s and annealing at 55 °C for 1 min. Absolute gene copy numbers were determined by the standard curve of 16S rRNA gene copy numbers. A single clone containing the

correct insert was grown in LB media and plasmid DNA was then extracted, purified and quantified. A 10-fold series of dilution of the plasmid DNA was then carried out to generate a standard curve covering six orders of magnitude from 10^3 to 10^8 copies of the template in the assay (Jing et al., 2017). All qPCRs were performed in technical duplicates. Blanks were always run with water instead of DNA extract. The final gene copy numbers were obtained by calibrating against total DNA content extracted from the soil. Seven genes involved in the denitrification process (*napA*, *narG*, *nirS*, *nirK*, *cnorB*, *qnorB* and *nosZ)* are included in this study (Table S1).

2.7. Calculations and statistical analysis

The cumulative gas emissions were calculated by linear interpolation between measured fluxes. Emission rates were expressed as arithmetic means of three replicates. Significance statistics were performed by Tukey's HSD test, following the homogeneity of variance, the tests of assumptions of normal distribution and one-way ANOVA. Statistical analyses were done using R (version 3.6.1), with $P < 0.05$ used as the criterion for statistical significance.

2.8. Data availability

All sequencing data associated with this study have been deposited at the NCBI Sequence Read Archive (SRA) under project accession number SRR12394466.

3. Results

3.1. Emissions of N_2O and N_2

General properties of the soils and sampling information is provided in Table 1. The initial soil nitrate concentrations ranged from 1.3 to 55.8 mg kg^{-1}, while at sites

A1042 (arid/semi-arid) and A2029 (hyperarid) the concentrations of nitrate were significantly higher than at the other sites (Table 1). In comparison, the initial ammonium concentrations were extremely low at all sites (0.04-0.5 mg kg^{-1} soil). At the end of the incubation cycle, the NO_3^- concentrations in soil had decreased, while the NH_4^+ concentrations showed an increase at all sites, with no significant difference observed among the sites ($P > 0.05$; Table 2).

The gas concentrations of all treatments were continuously monitored during the 60 days incubation experiment and the cumulative N_2O and N_2 emissions are shown in Fig. S1. The daily average N_2O and N_2 flux rates were characterized by four phases based on the different amendments (Fig. 1), i.e. water addition phase (day 0-34), nitrate addition phase (day 34-37), glucose addition phase (day 37-54) and anoxic phase (day 54-60). During the water addition phase, the N_2O fluxes ranged from 3.3 to 15.3 μg N_2O-N kg^{-1} d^{-1} in soils from all sites, with the highest flux rate seen in soils from site A1700, and the lowest from A2029. The N_2O fluxes remained low throughout the nitrate addition period (1.2-4.2 μg N_2O-N kg^{-1} d^{-1}), with no significant differences observed among the different locations. Pronounced N_2O emissions were observed after glucose addition in all locations (Fig. 1a), with significantly higher N_2O fluxes observed in soils from the A2029 site compared to those from the other sites. During the anoxic phase, the N_2O fluxes declined again in soils from all sites and ranged from 0.15 to 7.5 μg N_2O-N kg^{-1} d^{-1}.

N_2 emissions were below the detection limit during the water addition and nitrate addition phases, while pronounced N_2 emissions were detected in soils from all sites during the glucose addition phase (Fig. 1b). During the anoxic phase, N_2 emissions sharply increased to about 1500 μg N_2-N kg^{-1} d^{-1} and remained high until the end of the incubation. These emissions were ca. 5 times higher than the highest N_2O losses

seen after glucose addition. Similar N_2 responses were observed in samples from all sites.

3.2. N_2O SP_0 values and source partitioning

The SP_0 values for each of the measured points are provided in Table S3. The measured $\delta^{15}N^{sp}$ and $\delta^{18}O$ values of N_2O are presented in Figure 2a. The values for mixing endmembers between nitrification/fungal denitrification and bacterial denitrification yield the $\delta^{15}N^{sp}/\delta^{18}O$ slope for the mixing line, while the values for reduction isotope effects yield the $\delta^{15}N^{sp}/\delta^{18}O$ slope for the reduction line (Yu et al., 2020). The proportions of N_2O derived from bacterial denitrification were shown based on the two end-member model of the SP_0 value (Fig. 2b). In soils from the less arid sites (A1042 and A1700), a much lower contribution of bacterial denitrification was observed compared to the more arid sites (A2029 and A2116). Glucose addition appears to cause a significant N_2O reduction to N_2 effect in soils from all sites (Fig. 2a). Due to the extremely low N_2O concentrations (<200 ppb) measured for the hyperarid samples (A2029 and A2116), the SP_0 values could not be determined prior to glucose addition. Upon glucose addition, bacterial denitrification contributed more than 90% of the N_2O emission in soils from these two sites. Interestingly, in soils from the A1700 site, a clear increase of bacterial denitrification-derived N_2O (from ca. 50% to ca. 80%) was observed after glucose addition.

3.3. Microbial community composition and denitrification gene abundance

The DNA contents of soils before incubation were extremely low and ranged from 4.5 to 12.7 ng μL^{-1} (Table S2). These low DNA yields prevented the generation of high-quality PCR products. In contrast, at the end of the incubation, the DNA contents

of the soils had increased by 3~6 times and ranged from 18.4 to 36.5 ng μL^{-1} (Table S2). Rarefaction curves of assigned OTUs as a function of sequenced reads approached a plateau for most samples (Fig. S2), indicating that sufficient reads were obtained to cover most of diversity in the incubated soils. This is confirmed by Good's coverage values (at 97% similarity level), which were greater than 0.983 for all samples.

A diverse array of bacteria was observed in the incubated soils across the aridity gradient, categorized into 11 dominant phyla (Fig. 3). They were *Proteobacteria* (28.1-79.5%), *Actinobacteria* (6.1-26.8%), *Firmicutes* (4.2-27.5%), *Bacteroidetes* (4.8-9.1%), *Acidobacteria* (0.57-3.57%), *Armatimonadetes* (0.03-1.37%), *Planctomycetes* (0.25-1.03%), *Verrucomicrobia* (0.13-0.93%), *Chloroflexi* (0.09-0.54%), *Nitrospirae* (0.02-0.17%) and *Cyanobacteria* (0.03-0.13%), contributing to more than 96% of all OTUs.

Bacterial richness in the incubated soils clearly decreased with increasing aridity, as all three richness indices (PD, Chao1 and OTUs) decreased with increasing elevation along the transect (Table 3). The Shannon index also showed this decreasing trend with increasing aridity, but differences were not statistically significant (Table 3). Similarly, soils from a higher elevation had a lower number of taxa at class, order, family and OTU level resolution than soils from a lower elevation, while phylum and genus level data did not show differences. More specifically, the number of classes, orders and families at A2029 and A2116 were observed to be ca. 20% lower than those at A1042 and A1243 (Table 3).

Genes involved in the entire denitrification process were detected by qPCR in all incubated soils at the end of the incubation period, including *napA*, *narG*, *nirS*, *nirK*, *cnorB*, *qnorB* and *nosZ* (Fig. 4). Location along the aridity gradient had no impact on

the abundance of these genes.

4. Discussion

4.1. Denitrification potential in soils from the Atacama Desert

Overall, there is a paucity of research on the distribution of denitrifying organisms and their contribution to denitrification in desert ecosystems. This is surprising given the estimate that up to 30% of N_2 lost from terrestrial ecosystems originates from deserts (Bowden, 1986). These losses have been primarily attributed to denitrification (Orlando et al., 2012). Although denitrification is commonly believed to occur in moist soil, denitrifying organisms are able to thrive even in extreme environments (Glass and Silverstein, 1999). In soils of the Atacama Desert, denitrification-related genes have been detected, however, measurements of substrate-induced denitrification activity remained below the limit of detection (Orlando et al., 2012). Therefore, it has remained an unresolved question as to whether microorganisms recovered from most arid environments on Earth actually thrive under such extreme conditions or whether they are just dead or dying vestiges of viable cells fortuitously deposited by atmospheric processes. In our study, the DNA content of the unamended soils was too low to be amplified; however, after incubation of the soils with water, nitrate and glucose-C, DNA recovery was much greater indicating a relatively rapid growth of the microorganisms. In addition, a full complement of denitrification-related genes capable of transforming NO_3^- all the way to N_2 were detected in all our incubated soils (Fig. 4). Their functional significance is also confirmed by the observed measurements of N_2O and N_2 production. These facts indicated that the Atacama Desert can indeed provide a temporary, time-constrained habitat for denitrifying bacteria to thrive, possibly after transient fogs or rare rainfall events (Schulze-Makuch

et al., 2018; Meseguer-Ruiz et al., 2020). The denitrification potential in the Atacama soils (1420-1748 μg N kg^{-1} d^{-1}) was lower than reported denitrification potential rates for cropland and grassland ecosystems (4800-9600 μg N kg^{-1} d^{-1}) (Attard et al., 2011), but higher than in other desert ecosystems (0-521 μg N kg^{-1} d^{-1}) (Billings et al., 2002; McKeon et al., 2005; Orlando et al., 2012). It should be noted that most of the previous studies employed the acetylene inhibition technique for measuring the rate of soil denitrification potential, which may underestimate total soil denitrification (Nadeem et al., 2013). No clear trend was observed in terms of increasing aridity vs N_2O emission rates, possibly due to large difference in soil properties among the different sites. This indicates that other soil forming factors (e.g. parent material) rather that moisture may be driving denitrifier abundance in soil.

4.2. Relative contribution of fungal denitrification and bacterial denitrification

The contribution of fungi to N_2O emissions can vary widely from 17 to 89% (Xu et al., 2019). Using SP values and the two end-member approach enabled us to estimate the relative contributions of fungal and bacterial denitrification to N_2O emissions. However, this relies on the assumptions that i) the N_2O reduction fractionation effect on SP values can be corrected, and ii) N_2O derived from nitrification and nitrifier denitrification is negligible (Senbayram et al., 2018). With respect to the first point, we calculated the SP_0 using either a direct measurement of N_2 production or a $\delta^{15}N^{sp}/\delta^{18}O$ mapping model by considering the N_2O reduction fractionation effect (Lewicka-Szczebak et al., 2017). With regard to the second assumption, the extremely low NH_4^+ concentrations in our soils are unlikely to support large amounts of nitrification. We attribute these low concentrations not to biotic conversion of NH_4^+ to NO_3^- by nitrifiers but to abiotic losses of NH_4^+ as NH_3 due to the alkaline nature of

the soils (Jones et al., 2018). This suggests that N_2O emissions via nitrification are likely to be negligible, especially during the glucose addition phase. Thirdly, as shown in Figure 2a, most of the pre-glucose addition samples plotted near the bacterial denitrification-fungal denitrification mixing line. Therefore, based on our N_2O isotopomer data we estimate that about half of the N_2O production originated from fungal denitrification at the less arid sites (A1042 and A1700) before glucose addition, while bacterial denitrification dominated at the more arid sites (also for A1700 after glucose addition). Many fungal species are known to have denitrifying systems, of which *Cylindrocarpon tonkinense*, *Trichoderma* spp. and *Fusarium oxysporum* are deemed to be globally important (Shoun et al., 2012; Maeda et al., 2015). The latter has recently been detected in the rhizosphere and Llamara mats of the Atacama Desert (Gonzalez-Teuber et al., 2017; Santiago et al., 2018). The contribution of bacterial denitrification to N_2O emission appears to increase with increasing aridity, contributing up to 90% of total N_2O production at the most hyperarid sites. This is possibly due to greater competition from xerophilic fungi, which do not possess denitrification genes (Ochoa-Hueso et al., 2018). It has been shown that fungal communities show a stronger resistance to aridity than bacteria, while bacterial communities often display more resilience upon rewetting than fungal communities (Barnard et al., 2013). Furthermore, soil bacterial networks may link more strongly to soil functioning during recovery than fungal communities (de Vries et al., 2018). The dominance of bacterial denitrification-derived N_2O revealed that bacterial communities dominate N_2O production upon rewetting of arid soils. Our results support the view that bacteria may play a more important role in soil functioning resilience than the fungal community in an extreme environment, at least for N cycling.

401

402 *4.3. Soil microbial diversity and functionality in desert soils*

403 A loss of microbial biomass, reduction in biodiversity and simplification of soil
404 food webs can impair multiple ecosystem functions, including plant diversity,
405 decomposition, nutrient retention, and nutrient cycling (Wagg et al., 2014). Our
406 results show that increasing aridity reduces microbial diversity, consistent with
407 previous studies (Knief et al., 2020; Maestre et al., 2015). Further, the bacterial
408 richness and diversity in our soils was much lower than seen in other desert systems
409 (Zhang et al., 2019), croplands (Yao et al., 2020) and grassland (Raut et al., 2018)
410 (Table 3). The reduced bacterial richness in the Atacama soils, however, had no
411 impact on the capacity of the community to undertake full denitrification or on
412 potential denitrification rates (Fig. 1). There are at least two implications of this
413 finding. First, soil microbial function can be rapidly awakened even in extreme hostile
414 environments (Jones et al., 2018). Generally, the active microbial biomass only
415 constitutes about 0.1-2% of the total microbial biomass in soils where microbial
416 growth is constrained by a lack of water or available-C (Blagodatskaya and Kuzyakov,
417 2013). This ratio is expected to be much lower in the Atacama Desert where extreme
418 temperatures and low levels of available C and water constrain metabolic activity.
419 Most microbes exist in a dormant state and can rapidly recover with response to
420 substrate and moisture input (Jones and Murphy, 2007). Secondly, a fundamental
421 question of soil microbiology is to disentangle compositional versus environmental
422 effects on ecosystem function (Graham et al., 2016). One main message is that for
423 nutrient cycling, diversity effects are of most importance at the low end of the
424 diversity spectrum (Bardgett and van der Putten, 2014). Since common bacteria phyla,
425 *Proteobacteria*, *Actinobacteria*, *Firmicutes*, *Bacteroidetes*, *Acidobacteria*,

426 *Verrucomicrobia* etc. appeared in our soils after substrate incubation (Fig. 3), our
427 results further support the tenet that microbial composition is not the factor regulating
428 function, rather it is the prevailing environmental conditions, more exactly the
429 presence of substrate. Therefore, functional redundancy of microbial communities
430 could be even larger than originally thought for these types of extreme environments
431 (Wall and Virginia, 1999). This view is consistent with hyper-cold desert
432 environments (Wei et al., 2016). A meta-analysis of 111 experiments suggests that the
433 most species-rich polyculture tends to be no different functionally from that of the
434 single most productive species (Cardinale et al., 2006), which suggests that ecosystem
435 function may ultimately just be determined by certain (single) productive species.
436
437 *4.4. Implications for significant N_2O losses in the Atacama Desert*
438 The Atacama Desert currently holds about 250 Mt of nitrate deposits, hosted by a
439 complex mineral layer of 0.2-3 m thick (Reich and Bao, 2018). This is about twice the
440 global amount of N used annually for fertiliser application (Oyarzun and Oyarzun,
441 2007). Based on new evidence from mass-independent oxygen isotopic compositions,
442 the huge nitrate deposit in some parts of the Atacama Desert is found to be the result
443 of the absence of N loss processes and atmospheric deposition of particles produced
444 by gas to particle conversion, with minor but varying amounts from sea spray and
445 local terrestrial sources, while the major nitrate deposits could have accumulated from
446 atmospheric deposition in a period of 200,000 to 2.0 M years (Bull et al., 2016;
447 Michalski et al., 2004). Despite Atacama's extreme dryness, several extreme
448 precipitation events have struck regions of the Atacama Desert core during the last
449 five years, causing local flash flooding events (Wilcox et al., 2016; Azua-Bustos et al.,
450 2018; Schulze-Makuch et al., 2018). Since the soil denitrification functionality in the

Atacama Desert soil is able to recover shortly after water and C addition, the large reserves of nitrate stored in this desert ecosystem could potentially lead to significant N_2O emissions, resulting in a positive feedback to climate warming under those extreme meteorological events or land-use change scenario, while N_2 dominance is unlikely to occur due to the high nitrate content and low C status of the soil (Firestone and Davidson, 1989; Senbayram et al., 2018).

Acknowledgements

The authors thank Dr Lewicka-Szczebak for helping on the isotopomer mapping calculations. This work was funded by the ABCJ Geoverbund and the German Science Foundation (DFG) as part of CRC1211, the UK Natural Environment Research Council (Grant No. NE/M005143/1) and National Natural Science Foundation of China (Grants No. 41977045; 42077037).

References

Attard, E., Recous, S., Chabbi, A., Berranger, C. D., Guillaumaud, N., Labreuche, J., Philippot, L., Schmid, B., Roux, X. L., 2011. Soil environmental conditions rather than denitrifier abundance and diversity drive potential denitrification after changes in land uses. Global Change Biology 17, 1975–1989.

Azua-Bustos, A., Fairén, A. G., González-Silva, C., Ascaso, C., Carrizo, D., Fernández-Martínez, M. Á., Fernández-Sampedro, M., García-Descalzo, L., García-Villadangos, M., Martin-Redondo, M. P., Sánchez-García, L., Wierzchos, J., Parro, V., 2018. Unprecedented rains decimate surface microbial

communities in the hyperarid core of the Atacama Desert. Scientific Reports 8, 1–10.

Azua-Bustos, Armando, Urrejola, C., Vicuña, R., 2012. Life at the dry edge: Microorganisms of the Atacama Desert. FEBS Letters 586, 2939–2945.

Bardgett, R. D., van der Putten, W. H., 2014. Belowground biodiversity and ecosystem functioning. Nature 515, 505–511.

Barnard, R. L., Osborne, C. A., Firestone, M. K., 2013. Responses of soil bacterial and fungal communities to extreme desiccation and rewetting. The ISME Journal 7, 2229–2241.

Billings, S. A., Schaeffer, S. M., Evans, R. D., 2002. Trace N gas losses and N mineralization in Mojave desert soils exposed to elevated CO_2. Soil Biology & Biochemistry 34, 1777–1784.

Blagodatskaya, E., Kuzyakov, Y., 2013. Active microorganisms in soil: Critical review of estimation criteria and approaches. Soil Biology & Biochemistry 67, 192–211.

Bowden, W.B., 1986. Gaseous nitrogen emissions from undisturbed terrestrial ecosystems: an assessment of their impacts on local and global nitrogen budgets. Biogeochemistry 2, 249–279.

Bull, A. T., Asenjo, J. A., Goodfellow, M., Gómez-Silva, B., 2016. The Atacama Desert: Technical resources and the growing importance of novel microbial diversity. Annual Review of Microbiology 70, 215–234.

Calderón, R., Palma, P., Parker, D., Molina, M., Godoy, F. A., Escudey, M., 2014. Perchlorate levels in soil and waters from the Atacama Desert. Archives of Environmental Contamination and Toxicology 66, 155–161.

Caporaso, J. G., Kuczynski, J., Stombaugh, J., Bittinger, K., Bushman, F. D., Costello, E. K., Fierer, N., Peña, A. G., Goodrich, J. K., Gordon, J. I., Huttley, G. A., Kelley, S. T., Knights, D., Koenig, J. E., Ley, R. E., Lozupone, C. A., McDonald, D., Muegge, B. D., Pirrung, M., Knight, R., 2010. QIIME allows analysis of high-throughput community sequencing data. Nature Methods 7, 335–336.

Cardinale, B. J., Srivastava, D. S., Emmett Duffy, J., Wright, J. P., Downing, A. L., Sankaran, M., Jouseau, C., 2006. Effects of biodiversity on the functioning of trophic groups and ecosystems. Nature 443, 989–992.

de Vries, F. T., Griffiths, R. I., Bailey, M., Craig, H., Girlanda, M., Gweon, H. S., Hallin, S., Kaisermann, A., Keith, A. M., Kretzschmar, M., Lemanceau, P., Lumini, E., Mason, K. E., Oliver, A., Ostle, N., Prosser, J. I., Thion, C., Thomson, B., Bardgett, R. D., 2018. Soil bacterial networks are less stable under drought than fungal networks. Nature Communications 9, 3033.

Firestone, M., 1982. 8. Biological Denitrification. Nitrogen in Agricultural Soils, American Society of Agronomy, Inc. Crop Science Society of America, Inc. Soil Science Society of America Inc. Madison, WI, USA. pp. 289–326. DOI:10.2134/agronmonogr22

Frame, C. H., Casciotti, K. L., 2010. Biogeochemical controls and isotopic signatures of nitrous oxide production by a marine ammonia-oxidizing bacterium. Biogeosciences 7, 2695–2709.

Glass, C., Silverstein, J., 1999. Denitrification of high-nitrate, high-salinity wastewater. Water Research 33, 223–229.

Gonzalez-Teuber, M., Vilo, C., Bascunan-Godoy, L., 2017. Molecular characterization of endophytic fungi associated with the roots of *Chenopodium quinoa* inhabiting the Atacama Desert, Chile. Genomics Data 11, 109-112.

Graham, E.B., Knelman, J.E., Schindlbacher, A., Siciliano, S., Breulmann, M., Yannarell, A., Bemans, J.M., Abell, G., Philippot, L., Prosser, J., 2016. Microbes as Engines of Ecosystem Function: When Does Community Structure Enhance Predictions of Ecosystem Processes? Frontiers in Microbiology 7, 214.

Hoffmeister, D., 2018. Meteorological and soil measurements of the permanent master weather station 33 - Quebrada Grande, Chile [Data set]. CRC1211 Database CRC1211DB. DOI: 10.5880/CRC1211DB.1.

Jing, Z., Chen, R., Wei, S., Feng, Y., Zhang, J., Lin, X. 2017. Response and feedback of C mineralization to P availability driven by soil microorganisms. Soil Biology & Biochemistry 105, 111-120.

Jones, D.L., Murphy, D.V., 2007. Microbial response time to sugar and amino acid additions to soil. Soil Biology & Biochemistry 39, 2178-2182.

Jones, D. L., Olivera-Ardid, S., Klumpp, E., Knief, C., Hill, P. W., Lehndorff, E., Bol, R., 2018. Moisture activation and carbon use efficiency of soil microbial communities along an aridity gradient in the Atacama Desert. Soil Biology & Biochemistry 117, 68–71.

Knief, C., Bol, R., Amelung, W., Kusch, S., Frindte, K., Eckmeier, E., Jaeschke, A., Dunai, T., Fuentes, B., Mörchen, R., Schütte, T., Lücke, A., Klumpp, E., Kaiser, K., Rethemeyer, J., 2020. Tracing elevational changes in microbial life and organic carbon sources in soils of the Atacama Desert. Global and Planetary Change 184, 103078.

Köster, J. R., Cárdenas, L., Bol, R., Lewicka-Szczebak, D., Senbayram, M., Well, R., Giesemann, A., Dittert, K., 2015. Anaerobic digestates lower N_2O emissions compared to cattle slurry by affecting rate and product stoichiometry of denitrification – An N_2O isotopomer case study. Soil Biology & Biochemistry 84, 65–74.

Laughlin, R. J., Stenvens, R. J. 2002. Evidence for fungal dominance of denitrification and codenitrification in a grassland soil. Soil Science Society of America Journal 66, 1540–1548.

Lewicka-Szczebak, D., Well, R., Köster, J. R., Fuß, R., Senbayram, M., Dittert, K., Flessa, H., 2014. Experimental determinations of isotopic fractionation factors associated with N_2O production and reduction during denitrification in soils. Geochimica et Cosmochimica Acta 134, 55–73.

Maeda, K., Spor, A., Edel-Hermann, V., Heraud, C., Breuil, M.C., Bizouard, F., Toyoda, S., Yoshida, N., Steinberg, C., Philippot, L., 2015. N_2O production, a widespread trait in fungi. Scientific Reports 5, 9697.

Maestre, F. T., Delgado-Baquerizo, M., Jeffries, T. C., Eldridge, D. J., Ochoa, V., Gozalo, B., Quero, J. L., García-Gómez, M., Gallardo, A., Ulrich, W., Bowker, M. A., Arredondo, T., Barraza-Zepeda, C., Bran, D., Florentino, A., Gaitán, J., Gutiérrez, J. R., Huber-Sannwald, E., Jankju, M., Singh, B. K., 2015. Increasing aridity reduces soil microbial diversity and abundance in global drylands. Proceedings of the National Academy of Sciences 112, 15684–15689.

Mayol, E., Arrieta, J. M., Jiménez, M. A., Martínez-Asensio, A., Garcias-Bonet, N., Dachs, J., González-Gaya, B., Royer, S.-J., Benítez-Barrios, V. M., Fraile-Nuez, E., Duarte, C. M., 2017. Long-range transport of airborne microbes over the global tropical and subtropical ocean. Nature Communications 8, 1–9.

McKay, C. P., Friedmann, E. I., Gómez-Silva, B., Cáceres-Villanueva, L., Andersen, D. T., Landheim, R., 2003. Temperature and moisture conditions for life in the extreme arid region of the Atacama Desert: Four years of observations including the El Niño of 1997–1998. Astrobiology 3, 393–406.

McKeon, C. A., Jordan, F. L., Glenn, E. P., Waugh, W. J., Nelson, S. G., 2005. Rapid nitrate loss from a contaminated desert soil. Journal of Arid Environments 61, 119–136.

Meseguer-Ruiz, O., Cortesi, N., Guijarro, J.A., Sarricolea, P., 2020. Weather regimes linked to daily precipitation anomalies in Northern Chile. Atmospheric Research 236, 104802.

Michalski, G., Böhlke, J. K., Thiemens, M., 2004. Long term atmospheric deposition as the source of nitrate and other salts in the Atacama Desert, Chile: New evidence from mass-independent oxygen isotopic compositions. Geochimica et Cosmochimica Acta 68, 4023–4038.

Mörchen, R., Lehndorff, E., Diaz, F. A., Moradi, G., Bol, R., Fuentes, B., Klumpp, E., Amelung, W., 2019. Carbon accrual in the Atacama Desert. Global and Planetary Change 181, 102993.

Nadeem, S., Dörsch, P., Bakken, L. R., 2013. Autoxidation and acetylene-accelerated oxidation of NO in a 2-phase system: Implications for the expression of denitrification in ex situ experiments. Soil Biology & Biochemistry 57, 606–614.

Ochoa-Hueso, R., Collins, S. L., Delgado-Baquerizo, M., Hamonts, K., Pockman, W. T., Sinsabaugh, R. L., Smith, M. D., Knapp, A. K., Power, S. A., 2018. Drought consistently alters the composition of soil fungal and bacterial communities in grasslands from two continents. Global Change Biology 24, 2818–2827.

596 Orlando, J., Alfaro, M., Bravo, L., Guevara, R., Carú, M., 2010. Bacterial diversity
597 and occurrence of ammonia-oxidizing bacteria in the Atacama Desert soil
598 during a “desert bloom” event. Soil Biology and Biochemistry 42, 1183–1188.
599 Orlando, J., Carú, M., Pommerenke, B., Braker, G., 2012. Diversity and activity of
600 denitrifiers of Chilean arid soil ecosystems. Frontiers in Microbiology 3, 101.
601 Oyarzun, J., Oyarzun, R., 2007. Massive volcanism in the Altiplano-Puna volcanic
602 plateau and formation of the huge Atacama Desert nitrate deposits: A case for
603 thermal and electric fixation of atmospheric nitrogen. International Geology
604 Review 49, 962–968.
605 Philippot, L., Hallin, S., Schloter, M., 2007. Ecology of denitrifying prokaryotes in
606 agricultural soil. Advances in Agronomy 96, 249–305.
607 Quade, J., Rech, J. A., Latorre, C., Betancourt, J. L., Gleeson, E., Kalin, M. T. K.,
608 2007. Soils at the hyperarid margin: The isotopic composition of soil carbonate
609 from the Atacama Desert, Northern Chile. Geochimica et Cosmochimica Acta
610 71, 3772–3795.
611 Raut, S., Polley, H. W., Fay, P. A., Kang, S., 2018. Bacterial community response to a
612 preindustrial-to-future CO_2 gradient is limited and soil specific in Texas Prairie
613 grassland. Global Change Biology 24, 5815–5827.
614 Reich, M., Bao, H., 2018. Nitrate deposits of the Atacama Desert: A marker of
615 long-term hyperaridity. Elements 14, 251-256.
616 Santiago, I. F., Gonçalves, V. N., Gómez-Silva, B., Galetovic, A., Rosa, L. H., 2018.
617 Fungal diversity in the Atacama Desert. Antonie van Leeuwenhoek 111, 1345–
618 1360.
619 Schulze-Makuch, D., Wagner, D., Kounaves, S. P., Mangelsdorf, K., Devine, K. G.,
620 Vera, J.-P. de, Schmitt-Kopplin, P., Grossart, H.-P., Parro, V., Kaupenjohann,

M., Galy, A., Schneider, B., Airo, A., Frösler, J., Davila, A. F., Arens, F. L., Cáceres, L., Cornejo, F. S., Carrizo, D., Zamorano, P., 2018. Transitory microbial habitat in the hyperarid Atacama Desert. Proceedings of the National Academy of Sciences 115, 2670-2675.

Senbayram, M., Well, R., Bol, R., Chadwick, D. R., Jones, D. L., Wu, D., 2018. Interaction of straw amendment and soil NO_3^- content controls fungal denitrification and denitrification product stoichiometry in a sandy soil. Soil Biology & Biochemistry 126, 204–212.

Shoun, H., Fushinobu, S., Jiang, L., Kim, S.-W., Wakagi, T., 2012. Fungal denitrification and nitric oxide reductase cytochrome P450nor. Philosophical Transactions of the Royal Society B 367, 1186–1194.

Toyoda, S., Yoshida, N., 1999. Determination of nitrogen isotopomers of nitrous oxide on a modified isotope ratio mass spectrometer. Analytical Chemistry 71, 4711–4718.

Toyoda, S., Yoshida, N., Koba, K., 2017. Isotopocule analysis of biologically produced nitrous oxide in various environments. Mass Spectrometry Reviews 36, 135–160.

Uritskiy, G., Getsin, S., Munn, A., Gomez-Silva, B., Davila, A., Glass, B., Taylor, J., DiRuggiero, J., 2019. Halophilic microbial community compositional shift after a rare rainfall in the Atacama Desert. The ISME Journal 13, 2737–2749.

Valdivia-Silva, J. E., Navarro-González, R., Fletcher, L., Perez-Montaño, S., Condori-Apaza, R., Mckay, C. P., 2012. Soil carbon distribution and site characteristics in hyper-arid soils of the Atacama Desert: A site with Mars-like soils. Advances in Space Research 50, 108–122.

Wagg, C., Bender, S. F., Widmer, F., Heijden, M. G. A. van der., 2014. Soil biodiversity and soil community composition determine ecosystem multifunctionality. Proceedings of the National Academy of Sciences 111, 5266–5270.

Wall, D.H., Virginia, R.A., 1999. Controls on soil biodiversity: insights from extreme environments. Applied Soil Ecology 13, 137-150.

Walvoord, M. A., Phillips, F. M., Stonestrom, D. A., Evans, R. D., Hartsough, P. C., Newman, B. D., Striegl, R. G., 2003. A reservoir of nitrate beneath desert soils. Science 302, 1021–1024.

Warren-Rhodes, K. A., Rhodes, K. L., Pointing, S. B., Ewing, S. A., Lacap, D. C., Gómez-Silva, B., Amundson, R., Friedmann, E. I., McKay, C. P., 2006. Hypolithic cyanobacteria, dry limit of photosynthesis, and microbial ecology in the hyperarid Atacama Desert. Microbial Ecology 52, 389–398.

Wei, S.T.S., Lacap-Bugler, D.C., Lau, M.C.Y., Caruso, T., Rao, S., Rios, A.D.L., Archer, S.K., Chiu, J.M.Y., Higgins, C., Van Nostrand, J.D., Zhou, J.Z., Hopkins, D.W., Pointing, S.B., 2017. Taxonomic and functional diversity of soil and hypolithic microbial communities in Miers Valley, McMurdo Dry Valleys, Antarctica. Frontiers in Microbiology 7, 1642.

Wilcox, A. C., Escauriaza, C., Agredano, R., Mignot, E., Zuazo, V., Otárola, S., Castro, L., Gironás, J., Cienfuegos, R., & Mao, L. (2016). An integrated analysis of the March 2015 Atacama floods. Geophysical Research Letters, 43(15), 8035–8043.

Wu, D., Senbayram, M., Well, R., Brüggemann, N., Pfeiffer, B., Loick, N., Stempfhuber, B., Dittert, K., Bol, R., 2017. Nitrification inhibitors mitigate N_2O

emissions more effectively under straw-induced conditions favoring denitrification. Soil Biology & Biochemistry 104, 197–207.

Wu, D., Well, R., Cárdenas, L. M., Fuß, R., Lewicka-Szczebak, D., Köster, J. R., Brüggemann, N., Bol, R., 2019. Quantifying N_2O reduction to N_2 during denitrification in soils via isotopic mapping approach: Model evaluation and uncertainty analysis. Environmental Research 179, 108806.

Xu, H., Sheng, R., Xing, X., Zhang, W., Hou, H., Liu, Y., Qin, H., Chen, C., Wei, W., 2019. Characterization of fungal nirK-containing communities and N_2O emission from fungal denitrification in arable soils. Frontiers in Microbiology 10, 117.

Yao, T., Chen, R., Zhang, J., Feng, Y., Huang, M., Lin, X., 2020. Divergent patterns of microbial community composition shift under two fertilization regimes revealed by responding species. Applied Soil Ecology 154, 103590.

Yu, L., Harris, E., Lewicka□Szczebak, D., Barthel, M., Blomberg, M. R. A., Harris, S. J., Johnson, M. S., Lehmann, M. F., Liisberg, J., Müller, C., Ostrom, N. E., Six, J., Toyoda, S., Yoshida, N., Mohn, J., 2020. What can we learn from N_2O isotope data? Analytics, processes and modelling. Rapid Communications in Mass Spectrometry 34, e8858.

Zhang, K., Shi, Y., Cui, X., Yue, P., Li, K., Liu, X., Tripathi, B. M., Chu, H., 2019. Salinity is a key determinant for soil microbial communities in a desert ecosystem. MSystems 4, e00225-18.

Zheng, B., Zhu, Y., Sardans, J., Peñuelas, J., Su, J., 2018) QMEC: a tool for high-throughput quantitative assessment of microbial functional potential in C, N, P, and S biogeochemical cycling. Science China Life Sciences 61, 1451–1462.

694 Zhu, Y.-G., Zhao, Y., Li, B., Huang, C.-L., Zhang, S.-Y., Yu, S., Chen, Y.-S., Zhang,
695 T., Gillings, M. R., Su, J.-Q., 2017. Continental-scale pollution of estuaries with
696 antibiotic resistance genes. Nature Microbiology 2, 1–7.

697

698 **Table 1.** Properties of the soils along the elevational aridity gradient in the Atacama Desert.

Site name	**A1042**	**A1243**	**A1700**	**A2029**	**A2116**
Longitude	70°23'37.78"W	70°22'11.65"W	70°18'47.65"W	70°18'45.46"W	70°15'18.02"W
Latitude	25°00'46.67"S	25°01'19.23"S	24°59'18.32"S	24°56'59.45"S	25°02'38.01"S
Sand (%)	70.2	81.4	69	69.1	72.7
Silt (%)	24.3	15.6	25.4	10.1	19.5
Clay (%)	4.7	5.0	4.8	19.7	5.0
Distance to coast (km)	7.6	10.1	16.2	20.3	22.9
Elevation (m)	1042	1243	1703	2029	2116
pH	7.91	7.85	7.28	7.23	7.29
MAP (mm)	2	0	0	0	0
MAT (□)	18.0	17.6	16.7	16.7	16.7
TOC (%)	0.07±0.01	0.07±0.01	0.04±0.00	0.04±0.00	0.04±0.00
Total C (%)	0.85±0.39	0.66±0.27	0.06±0.00	0.06±0.00	0.11±0.02
NO_3^- (mg kg^{-1})	17.9±3.7	4.2±0.8	1.3±0.6	55.8±20.4	3.9±0.7
NH_4^+ (mg kg^{-1})	0.3±0.0	0.1±0.0	0.04±0.0	0.5±0.0	0.2±0.0

699 MAP, mean annual precipitation; MAT, mean annual temperature; TOC, total organic C. The soil texture, soil pH and distance to coast (km) is from
700 (Mörchen et al., 2019); MAP and MAT is from Quade et al. (2007) and Hoffmeister (2018). Data of TOC, total C, NO_3^- and NH_4^+ are means of three
701 replicates with standard error.

Table 2. Soil nitrate (NO_3^-) and ammonium (NH_4^+) concentrations at the end of the incubation experiment.

Site	**NO_3^- (mg kg^{-1} dry soil)**	**NH_4^+ (mg kg^{-1} dry soil)**
A1042	0.34±0.06	2.33±0.22
A1243	0.31±0.06	0.66±0.04
A1700	0.05±0.03	0.47±0.04
A2029	2.68±2.64	1.29±0.82
A2116	0.13±0.04	0.52±0.15

Data are means of three replicates with standard error.

710 **Table 3.** Bacterial richness in soils from different elevations along the transect after incubation

Site	Diversity indices				Observed number					Rarefied to	Ref.
	PD	Chao1	OTUs	Shannon	Phylum	Class	Order	Family	Genus		
A1042	48.96 a	925.2 a	692.7 a	4.33 a	20.0 a	50.3 a	75.3 a	132.3 a	217.3 a	15000	Current study
A1243	45.52 ab	877.9 a	623.3 ab	3.96 a	19.0 a	48.7 ab	73.3 a	130.0 a	217.7 a		
A1700	38.21 ab	744.2 ab	508.7 bc	3.89 a	19.3 a	44.0 ab	65.3 ab	116.7 ab	185.3 a		
A2029	35.12 b	733.8 ab	467.3 c	3.70 a	17.0 a	41.3 b	61.7 b	110.7 b	187.7 a		
A2116	35.25 b	682.7 b	452.7 c	3.62 a	19.3 a	44.3 ab	67.0 ab	120.0 ab	192.0 a		
Desert	147~91	/	3750~2000	/	/	/	/	/	/	27000	Zhang et al. (2019)
Cropland	/	2954	/	4.94	/	/	/	/	/	10000	Yao et al. (2020)
Grassland	190~285	/	/	6.5~7.5	47	141	222	259	/	20000	Raut et al. (2018)

All samples were rarefied to 15000 sequences per sample to evaluate the diversity indices. PD, Phylogenetic diversity index; Chao 1, Chao1 richness index; OTUs, observed OTUs; Shannon, Shannon index. Observed numbers of taxonomic categories were counted according to the taxonomic assignment of OTUs. Different letters in the same column denote significant differences among samples from the five different elevations ($p<0.05$, ANOVA-Tukey's HSD).

Figure captions

Fig. 1. Soil mean daily N_2O (a) and N_2 (b) emissions for 5 sites along a hyperaridity gradient in the Atacama Desert. The aridity gradient runs from left to right for the 5 sites (A1042 → A2116). Error bars show the standard error of each treatment (n = 3).

Fig. 2. (a) N_2O isotope data of incubation experiments in SP/O Map presented with literature endmember median values and theoretical mixing and reduction lines (Yu et al., 2020). $\delta^{18}O$ values of mixing endmembers bacterial denitrification and fungal denitrification are presented in relation to the mean measured ambient water ($\delta^{18}O$ of -6.4‰). Ranges of endmember values (standard deviation of mean values) are shown as boxes; (b) The proportion of bacterial denitrification derived N_2O based on N_2O ^{15}N site preference value in different phases. Note, part of the data is missing due to the extremely low N_2O concentrations (<200 ppb) where the SP_0 values could not be accurately determined.

Fig. 3. Relative abundance of the dominant bacterial taxonomic groups for 5 sites along a hyperaridity gradient in the Atacama Desert. Community structure was analyzed at the end of the incubation study. The aridity gradient runs from left to right for the 5 sites (A1042 → A2116). Data are means of three replicates.

Fig. 4. Abundance of genes involved in denitrification for 5 sites along a hyperaridity gradient in the Atacama Desert. Gene abundance was measured at the end of the

incubation study. The aridity gradient runs from left to right for the 5 sites (A1042 → A2116). Gene abundance data are means of three replicates with standard deviation.

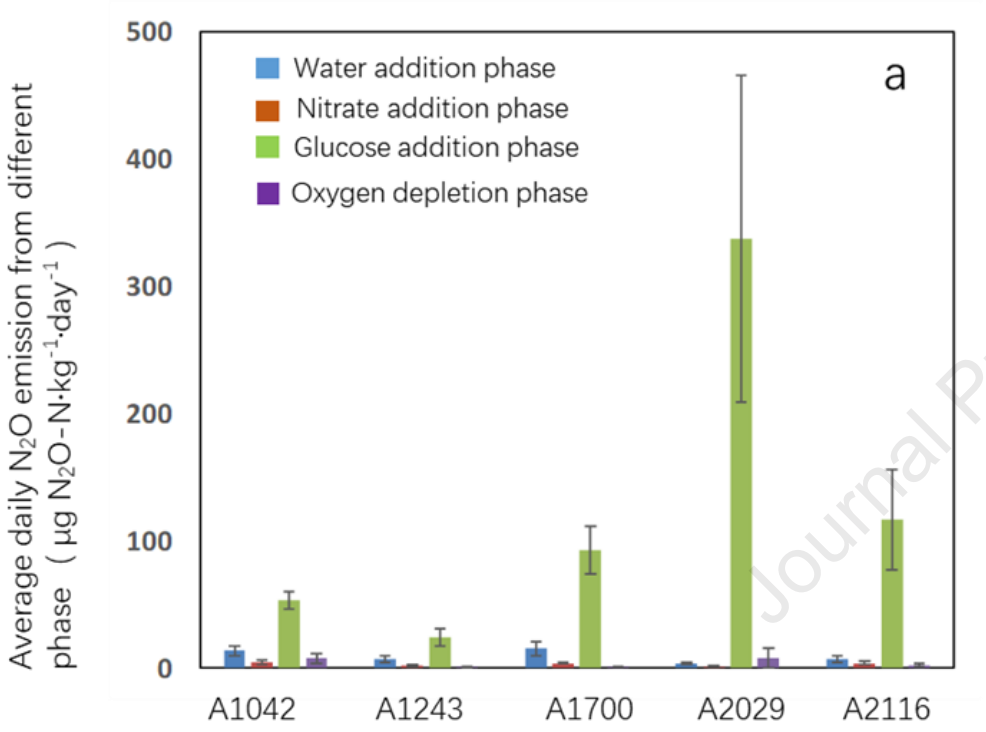

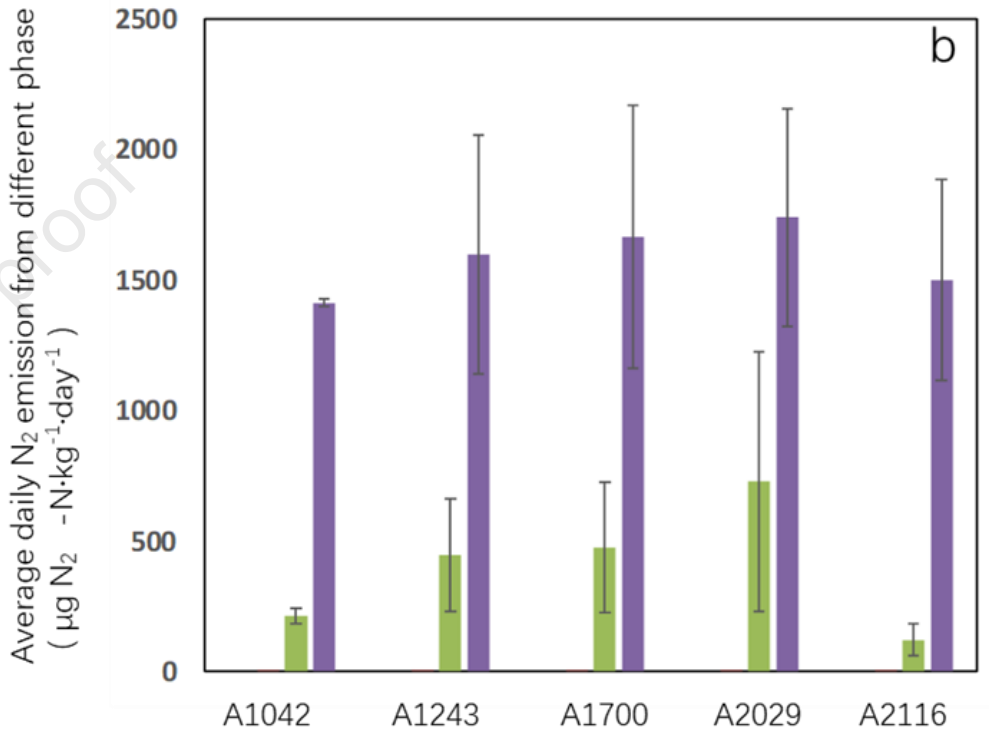

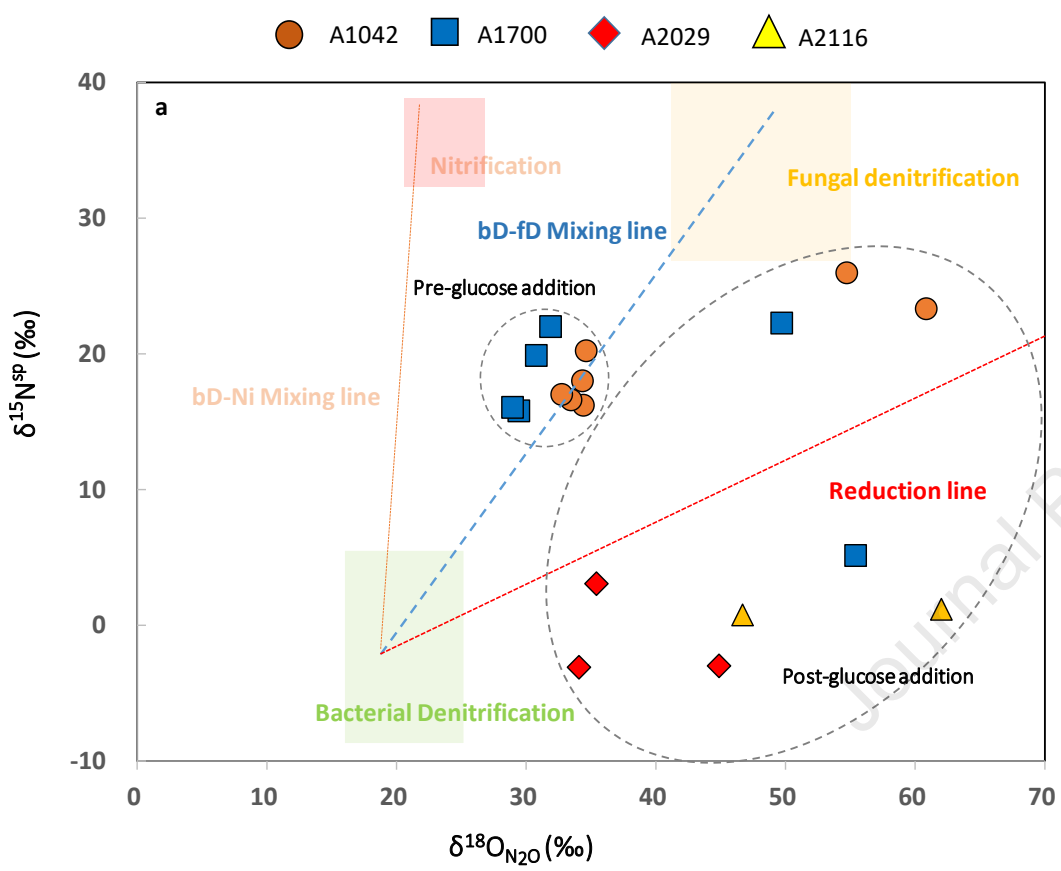

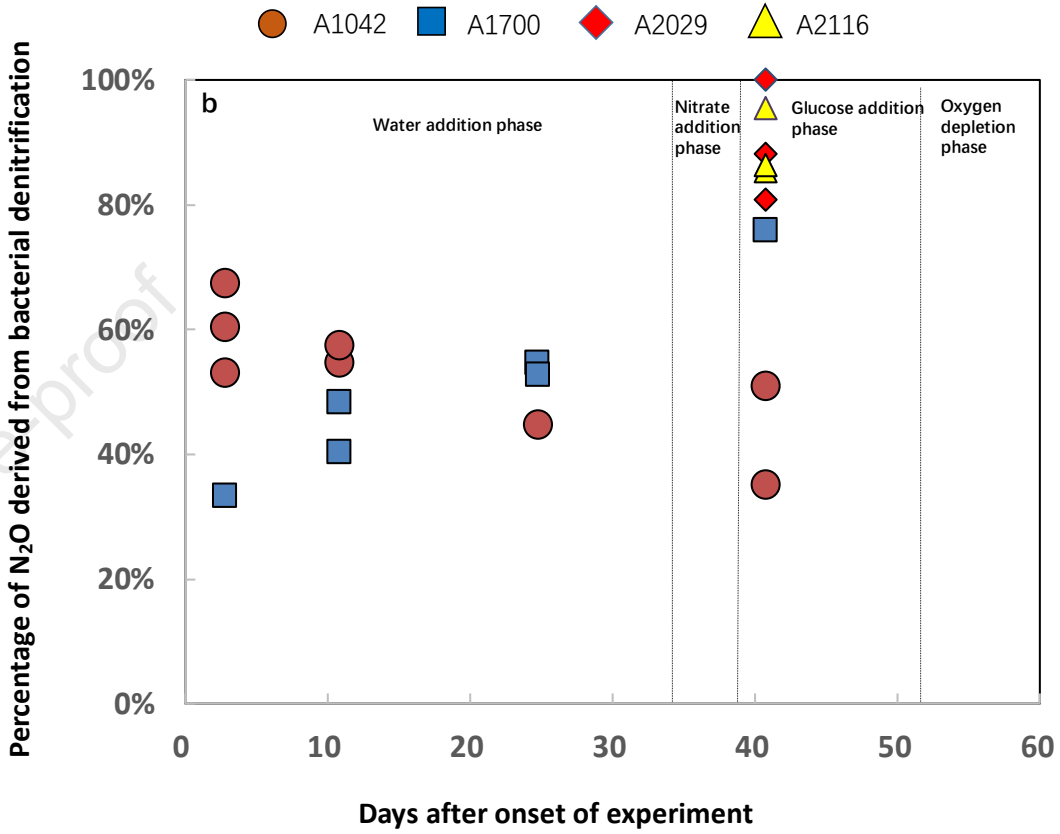

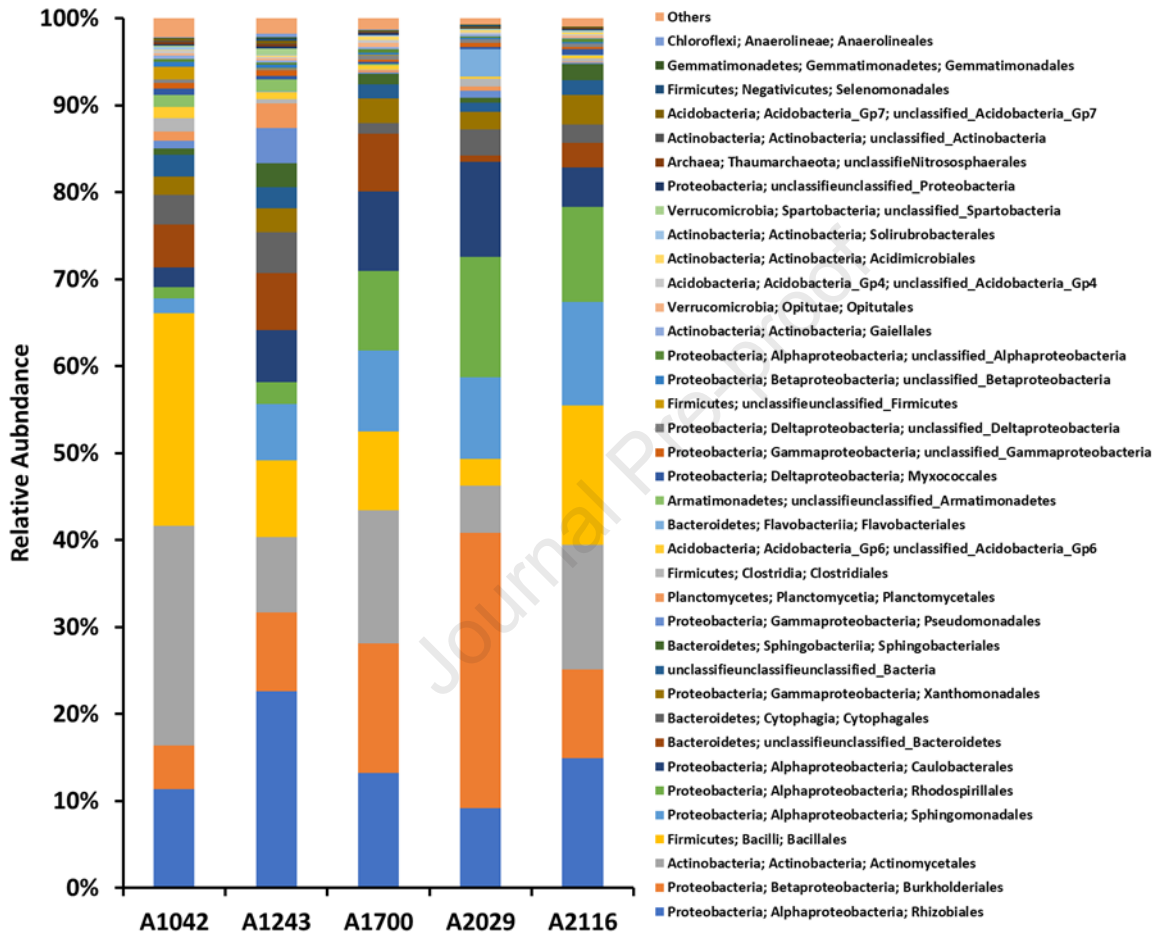

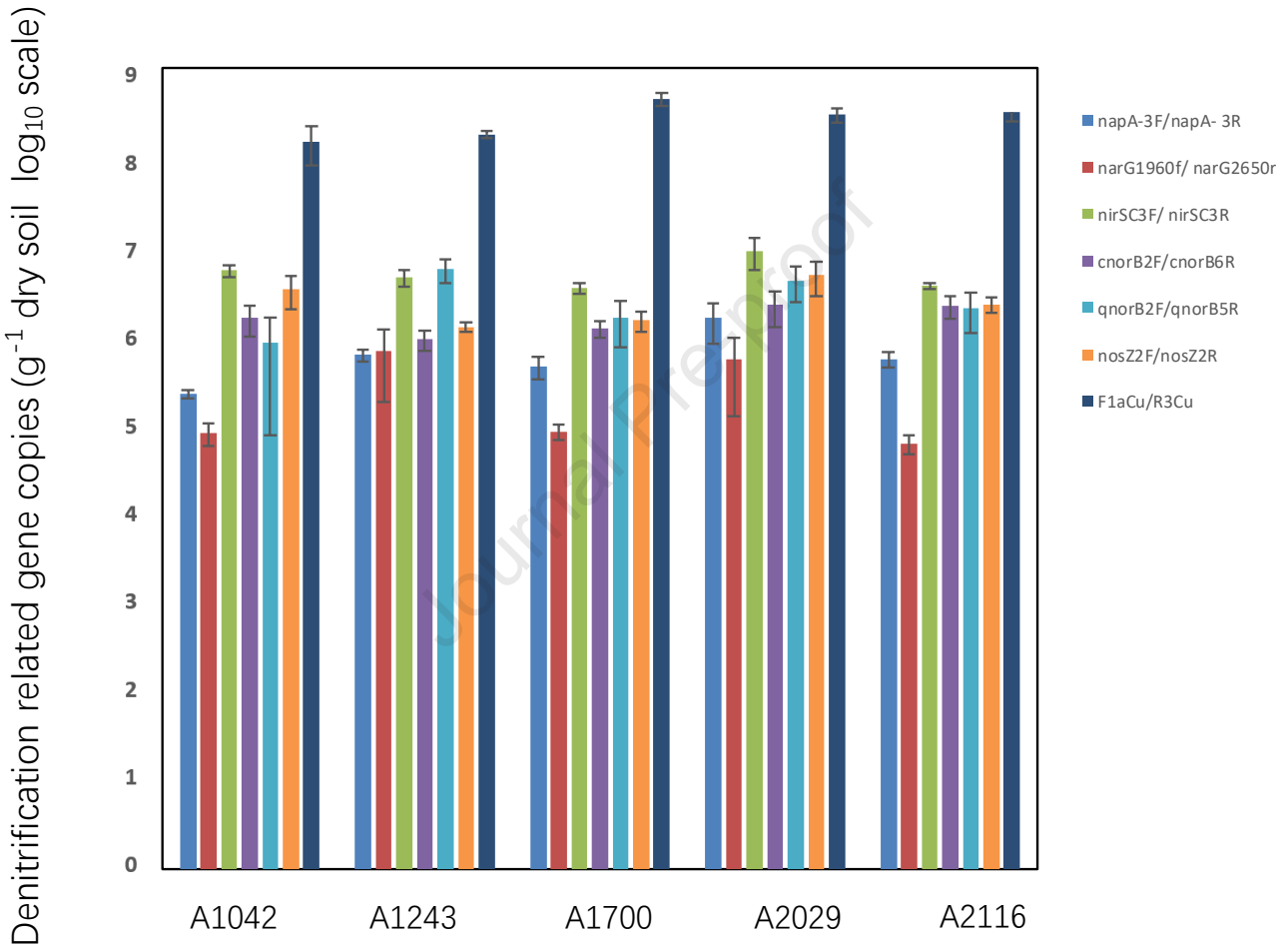

Highlights

i) Denitrification was shown to occur in the hyperarid Atacama Desert.

ii) Denitrification potential and associated gene abundance was not affected by aridity.

iii) Increasing aridity reduced soil bacterial richness.

iv) Fungal and bacterial denitrification co-contributed to N_2O production.

v) Bacterial denitrification dominated N_2O production with increasing hyperaridity.

Declaration of interests

☒ The authors declare that they have no known competing financial interests or personal relationships that could have appeared to influence the work reported in this paper.

☐The authors declare the following financial interests/personal relationships which may be considered as potential competing interests: